Reliability Analysis of High-Rise Buildings under Wind Loads

Ming-Yi Liu[1] and Yu-Jie Li[2]

[1]*Department of Civil Engineering, Chung Yuan Christian University, Jhongli City, Taoyuan County 32023, Taiwan, myliu@cycu.edu.tw*

[2]*Department of Civil Engineering, Chung Yuan Christian University, Jhongli City, Taoyuan County 32023, Taiwan, g9772001@cycu.edu.tw*

Abstract: The objective of this paper is to conduct the reliability analysis of high-rise buildings under wind loads. Numerical examples are provided to capture the dynamic effects of structures with eccentricity between the elastic and mass centers. The framework of this research consists of two stages. The first stage includes two parts: the deterministic analysis of wind-induced acceleration for a variety of attack angles, i.e., the demand, and the determination of allowable acceleration based on the occupant comfort criteria for wind-excited buildings, i.e., the capacity. According to the results obtained in the first stage, the reliability analysis is conducted in the second stage, which can predict the probability of dissatisfaction with occupant comfort criteria for a variety of probability distributions of the structural eccentricity. The findings indicate that, compared to the lognormal and type I extreme value distributions, the normal distribution can be used to more conservatively simulate the uncertainties of the eccentricity between the elastic and mass centers. Furthermore, the probability of dissatisfaction with occupant comfort criteria of the torsionally coupled system is relatively higher than that of the torsionally uncoupled system for each attack angle due to the coupled mode effects.

Keywords: Reliability analysis, High-rise building, Wind load, Elastic center, Attack angle

1. Introduction

Traditionally, structural analysis is based on deterministic approaches, i.e., each parameter of analytical model is considered to be a certain value. In fact, uncertainties exist in design, construction, operation and maintenance of real structures. Consequently, traditional analysis is not able to effectively capture structural properties. On the basis of probabilistic approaches, reliability analysis is used to simulate probability distribution of each parameter, implying that uncertainties can be reasonably modeled by such method. This fact indicates that reliability analysis is a more appropriate tool than traditional analysis. In Taiwan, both structural safety and occupant comfort of high-rise buildings have become important due to frequent typhoons, implying that wind hazard is a significant factor for design purposes. Uncertainties of both wind loads and high-rise buildings have to be considered for structural design. From the above description, reliability analysis is useful for exploring the problem of high-rise buildings under wind loads.

The objective of this paper is to conduct the reliability analysis of high-rise buildings under wind loads. Numerical examples are provided to capture the dynamic effects of structures with eccentricity between the elastic and mass centers. The framework of this research consists of two stages, as shown in Figure 1. The first stage includes two parts: the deterministic analysis of wind-induced acceleration for a variety of attack angles, i.e., the demand, and the determination of allowable acceleration based on the occupant comfort

5th International Conference on Reliable Engineering Computing (REC 2012)
Edited by M. Vořechovský, V. Sadílek, S. Seitl, V. Veselý, R. L. Muhanna and R. L. Mullen

ISBN 978-80-214-4507-9. Published by Ing. Vladislav Pokorný − LITERA

criteria for wind-excited buildings, i.e., the capacity. According to the results obtained in the first stage, the reliability analysis is conducted in the second stage, which can predict the probability of dissatisfaction with occupant comfort criteria for a variety of probability distributions of the structural eccentricity.

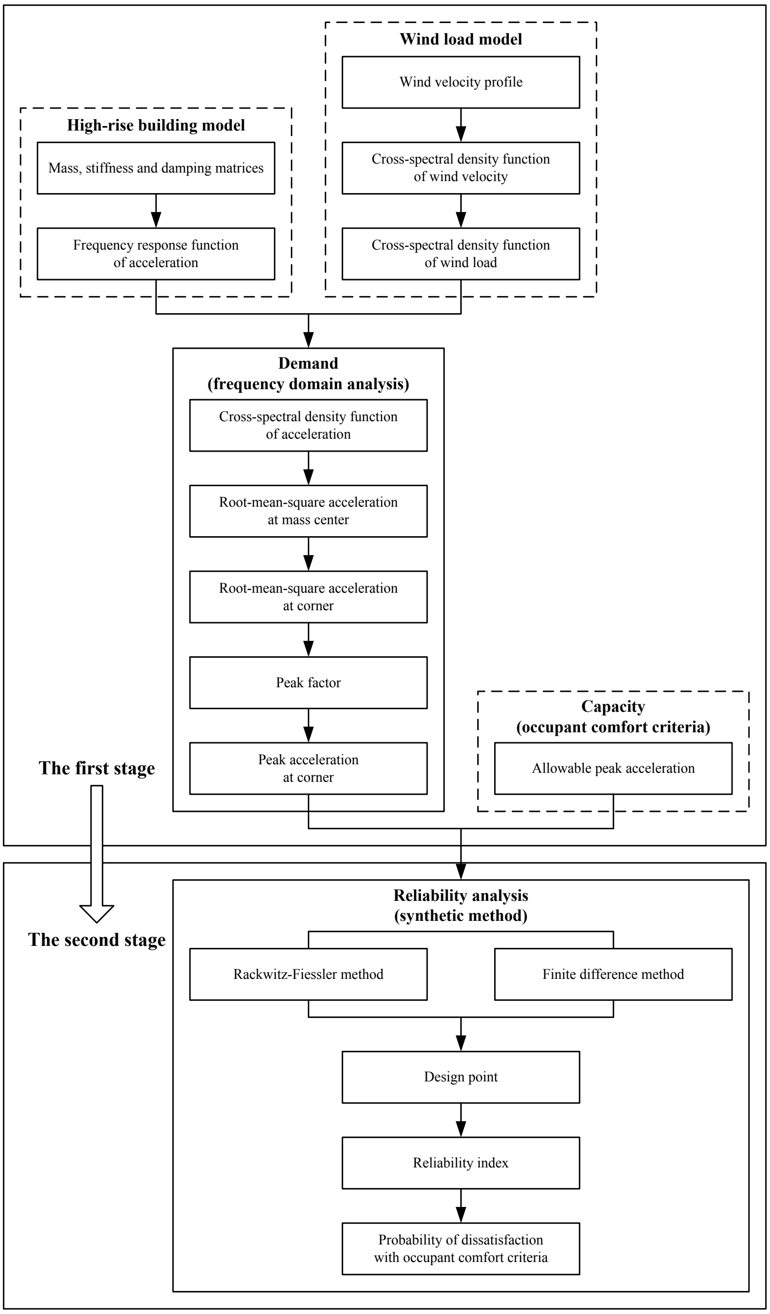

Figure 1. Framework of the research.

2. High-Rise Building Model

An N -story torsionally coupled system is used to simulate a high-rise building, and its corresponding three-dimensional configuration and top view of the i th floor are illustrated in Figure 2(a) and 2(b), respectively[1], where x, y, z and θ are the coordinates of the system; D_i, B_i, H_i and Z_i are the depth, breadth, height and elevation, respectively; MC_i, EC_i and AC_i are the mass, elastic and aerodynamic centers, respectively; Ex_i and Ey_i are the eccentricities between EC_i and MC_i in the x and y axes, respectively; Ax_i and Ay_i are the eccentricities between AC_i and MC_i in the x and y axes, respectively. Several assumptions are adopted in this study: (1) each rigid diaphragm with three degrees of freedom x_i, y_i and θ_i is characterized by the mass M_i and the moment of inertia I_i about MC_i; (2) each massless column is characterized by Kx_i, Ky_i and $K\theta_i$, which individually denote the stiffnesses in the x, y and θ axes referred to EC_i; (3) wind loads are applied at AC_i; (4) MC_i, EC_i and AC_i are non-coincident, and MC_i is located in the centroid of the diaphragm; (5) the Rayleigh damping with the mass-related coefficient A_0 and the stiffness-related coefficient A_1 is used. The model in Figure 2 can be simplified to an N -story torsionally uncoupled system when Ex_i and Ey_i both equal zero.

The procedure for the modeling of high-rise buildings is summarized in Figure 1. Based on the parameters mentioned above, the mass, stiffness and damping matrices of the system can be generated, and the frequency response function of acceleration can therefore be obtained (Kan and Chopra, 1977; Yang et al., 1981; Samali et al., 1985; Kareem, 1985; Kareem, 1992; Wu and Yang, 2000; Liu et al., 2008).

3. Wind Load Model

Wind loads can be decomposed into an average, aerodynamic damping and fluctuation terms. The fluctuation term is considered and the other two terms are neglected, which can be used to appropriately conduct the dynamic analysis under the assumption of small deformation theory. The wind load components including the drag, lift and torque are illustrated in Figure 3, where the attack angle ϕ is defined as the angle between the wind direction and the x axis. The drag and lift both act through AC_i, where the former and the latter are parallel and perpendicular to the wind direction, respectively. The torque is due to the eccentricity between AC_i and MC_i. The drag, lift and torque can be written as a function of ϕ (Yang et al., 1981; Samali et al., 1985; Wu and Yang, 2000; Simiu and Scanlan, 1996; Peng, 2005).

The procedure for the computation of wind loads is summarized in Figure 1. According to the power law, the wind velocity profile showing the variations in the mean wind velocity over the elevation can be expressed as a function of the exponent α, the gradient height Z_G and the gradient wind velocity V_G (Simiu and Scanlan, 1996). Based on the wind velocity profile, the reference mean wind velocity at 10 m above the ground V_R, the ground roughness coefficient K_0 and the exponential decay coefficient C_1 are used to calculate the cross-spectral density function of wind velocity between two elevations (Davenport,

[1] The subscript i in Figure 1 represents the parameter of the i th floor in this research.

1968). By combining both the wind velocity profile and cross-spectral density function of wind velocity, the cross-spectral density function of wind load between two axes can be obtained by the air density ρ, the windward side area of floor, the mean wind velocity, the drag coefficient C_D, the lift coefficient C_L, Ax_i and Ay_i for a variety of ϕ (Yang et al., 1981; Samali et al., 1985; Wu and Yang, 2000).

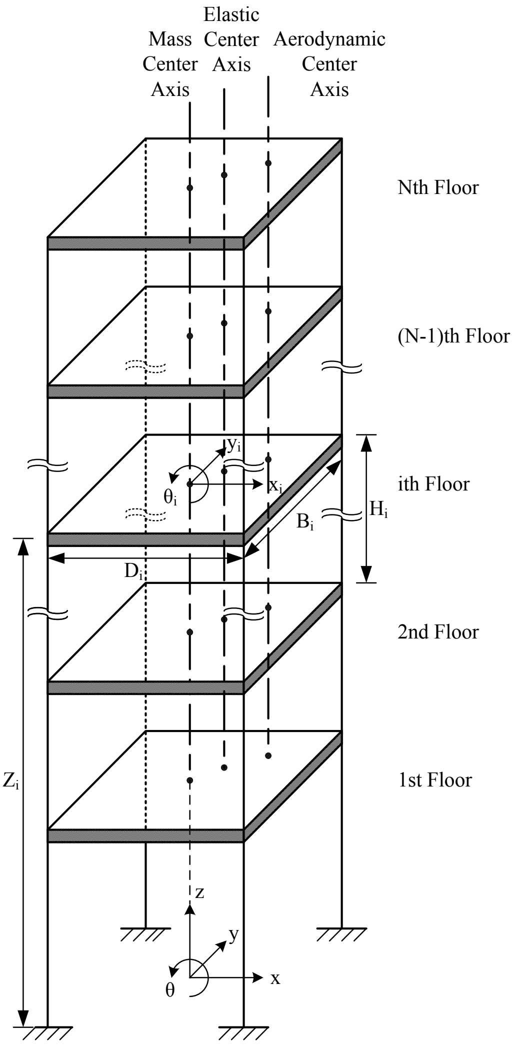

(a) Three-dimensional configuration

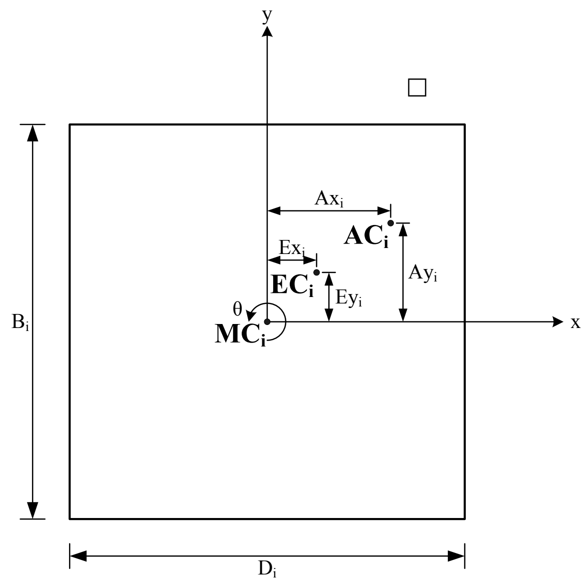

(b) Top view of the i th floor

Figure 2. N-story torsionally coupled system.

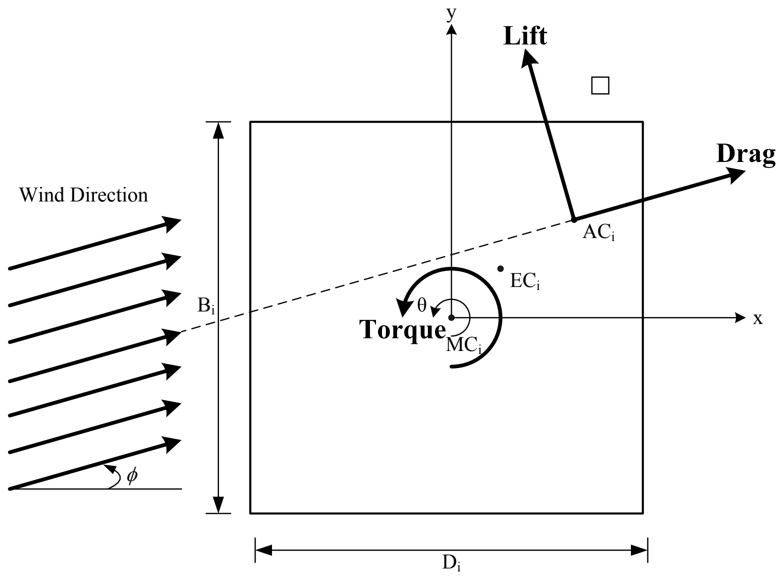

Figure 3. Wind load components.

4. Demand and Capacity

As shown in Figure 1, the deterministic analysis of wind-induced acceleration of structures with eccentricity between EC_i and MC_i for a variety of ϕ is conducted from the high-rise building and wind load models. The computational procedure is based on the frequency domain analysis. By combining both the frequency response function of acceleration and cross-spectral density function of wind load, the cross-spectral density function of acceleration between two axes, and the corresponding root-mean-square acceleration at mass center and that at corner can be calculated (Kareem, 1985; Kareem, 1992). The peak acceleration at corner, i.e., the demand, then can be obtained by multiplying the response at mass center by the peak factor (Melbourne, 1977).

The allowable peak acceleration of structures, i.e., the capacity, can be determined based on the occupant comfort criteria for wind-excited buildings. The threshold can be written as a function of the frequency of structural oscillation F, the duration of wind velocity T and the return period of wind velocity R (Melbourne and Palmer, 1992).

5. Reliability Analysis

According to the demand and capacity for different attack angles obtained in the first stage, the reliability analysis of high-rise buildings under wind loads based on the synthetic method combining both the Rackwitz-Fiessler and finite difference methods is conducted in the second stage, which can predict the design point, reliability index and probability of dissatisfaction with occupant comfort criteria for a variety of probability distributions of the structural eccentricity, as shown in Figure 1.

The basic variables X_i ($i = 1,2,\cdots,n$) and the corresponding limit state function $Z = g(X_1, X_2, \cdots, X_n)$ are the essences of reliability analysis. X_i ($i = 1,2,\cdots,n$) can be used to simulate the uncertainties of n parameters in a system. Z is the standard to judge whether each performance criterion is satisfied in the system. Figure 4(a) illustrates the relationships between Z and X_i ($i = 1,2,\cdots,n$) in the original coordinate system. The limit state ($Z = 0$) is the boundary between the safe region ($Z > 0$) and the unsafe region ($Z < 0$). X_i ($i = 1,2,\cdots,n$) can be transformed to the standard normal variables X'_i ($i = 1,2,\cdots,n$), respectively, and the corresponding limit state function $Z = g(X'_1, X'_2, \cdots, X'_n)$ can therefore be determined. The relationships between Z and X'_i ($i = 1,2,\cdots,n$) in the transformed coordinate system are illustrated in Figure 4(b). The safe region ($Z > 0$) and the unsafe region ($Z < 0$) are divided by the limit state ($Z = 0$) similar to Figure 4(a). The design point $(x_1'^*, x_2'^*, \cdots, x_n'^*)$[2] is located in $Z = 0$ closest to the origin. The reliability index β with the distance between the design point and the origin is a useful index for assessing the system reliability. The probability of dissatisfaction with occupant comfort criteria p_f can be expressed as a function of β (Haldar and Mahadevan, 2000a; Haldar and Mahadevan, 2000b).

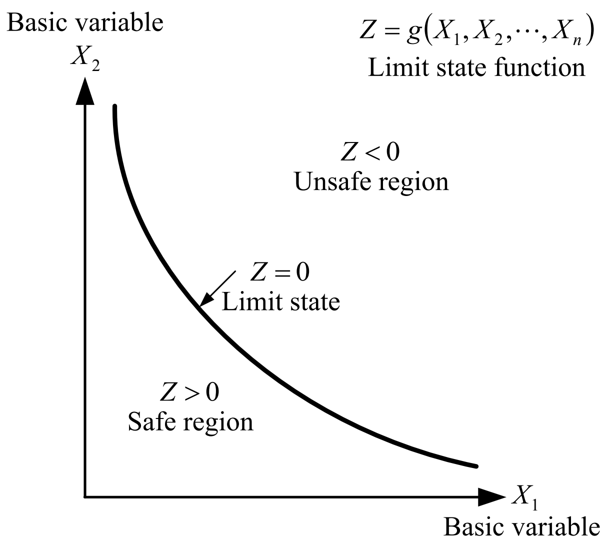

(a) Original coordinate system

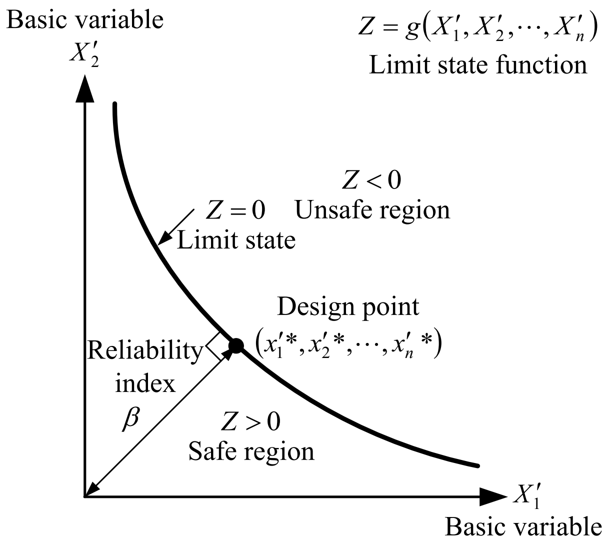

(b) Transformed coordinate system

Figure 4. Relationships between the limit state function and the basic variables.

The Rackwitz-Fiessler method contains the parameters in both the original and transformed coordinate systems. The algorithm is formulated as follows (Rackwitz and Fiessler, 1978):

[2] The parameters marked with asterisk represent the ones based on the design point in this research.

Step 1. Z is defined.

Step 2. The initial value for each component of the design point in the original coordinate system $x_i*(i=1,2,\cdots,n)$ is given. These values are assumed to be μ_{X_i} ($i=1,2,\cdots,n$) representing the mean values of X_i ($i=1,2,\cdots,n$), respectively. The corresponding initial value of $g(x_1*,x_2*,\cdots,x_n*)$ can therefore be determined.

Step 3. For the non-normal variables in X_i ($i=1,2,\cdots,n$), both their mean values and standard deviations of the equivalent normal variables, i.e., $\mu_{X_i}^N$ and $\sigma_{X_i}^N$ ($i=1,2,\cdots,n$), respectively, can be estimated based on the Rackwitz-Fiessler transformation (Rackwitz and Fiessler, 1976). $x_i'*(i=1,2,\cdots,n)$ then can be calculated as

$$x_i'*=\frac{x_i*-\mu_{X_i}^N}{\sigma_{X_i}^N}. \tag{1}$$

Step 4. $\left(\frac{\partial g}{\partial X_i}\right)^*$ ($i=1,2,\cdots,n$) are calculated.

Step 5. $\left(\frac{\partial g}{\partial X_i'}\right)^*$ ($i=1,2,\cdots,n$) can be calculated as

$$\left(\frac{\partial g}{\partial X_i'}\right)^*=\left(\frac{\partial g}{\partial X_i}\right)^*\sigma_{X_i}^N. \tag{2}$$

Step 6. $x_i'*(i=1,2,\cdots,n)$ can be modified by the recursive formula

$$New(x_1'*,x_2'*,\cdots,x_n'*)=\left[\frac{\sum_{i=1}^{n}\left(\frac{\partial g}{\partial X_i'}\right)^* x_i'*-g(x_1*,x_2*,\cdots,x_n*)}{\sum_{i=1}^{n}\left(\frac{\partial g}{\partial X_i'}\right)^{2*}}\right]\left[\left(\frac{\partial g}{\partial X_1'}\right)^*,\left(\frac{\partial g}{\partial X_2'}\right)^*,\cdots,\left(\frac{\partial g}{\partial X_n'}\right)^*\right]. \tag{3}$$

Step 7. β can be calculated as

$$\beta=\sqrt{\sum_{i=1}^{n}(x_i'*)^2}, \tag{4}$$

indicating that its value is equal to the distance between $(x_1'*,x_2'*,\cdots,x_n'*)$ and the origin. The convergence tolerance for β is assigned.

Step 8. Eq. (1) can be rewritten as

$$x_i^* = \mu_{X_i}^N + \sigma_{X_i}^N x_i'^*, \tag{5}$$

implying that x_i^* ($i = 1,2,\cdots,n$) are modified and $g(x_1^*, x_2^*, \cdots, x_n^*)$ can therefore be redetermined. The convergence tolerance for $g(x_1^*, x_2^*, \cdots, x_n^*)$ is assigned. Steps 3 to 8 are repeated until the convergence tolerances for both β and $g(x_1^*, x_2^*, \cdots, x_n^*)$ are achieved.

Eqs. (1), (2) and (5) will also be valid for the normal variables in X_i ($i = 1,2,\cdots,n$) if $\mu_{X_i}^N$ and $\sigma_{X_i}^N$ are replaced by their mean values μ_{X_i} and standard deviations σ_{X_i} ($i = 1,2,\cdots,n$), respectively. p_f can be approximately estimated based on the convergent β.

The finite difference method used herein is a perturbation-based approach. The computational procedure is summarized as follows (Haldar and Mahadevan, 2000b):

Step 1. The initial values of X_i, i.e., X_i^0 ($i = 1,2,\cdots,n$), are assumed to be μ_{X_i} ($i = 1,2,\cdots,n$), respectively. The corresponding value of Z before perturbation can therefore be determined as

$$Z_0 = g(X_1^0, X_2^0, \cdots, X_n^0). \tag{6}$$

Step 2. The small and positive ΔX_1 with respect to the perturbation of X_1 is given. ΔX_1 is assumed to be proportional to σ_{X_1}. X_1^0 is replaced by $X_1^0 + \Delta X_1$ and X_i^0 ($i = 2,3,\cdots,n$) remain the previous values. The corresponding value of Z after perturbation can therefore be determined as

$$Z_1 = g(X_1^0 + \Delta X_1, X_2^0, \cdots, X_n^0). \tag{7}$$

Step 3. The difference of Z before and after perturbation can be calculated as

$$\Delta Z = Z_1 - Z_0. \tag{8}$$

The derivative of Z with respect to X_1 can be approximately estimated as $\dfrac{\Delta Z}{\Delta X_1}$.

Step 4. Similarly, the derivatives of Z with respect to X_i ($i = 2,3,\cdots,n$) can also be approximately obtained as $\dfrac{\Delta Z}{\Delta X_i}$ ($i = 2,3,\cdots,n$), respectively, by repeating Steps 2 and 3.

By individually substituting $g\left(X_1^0, X_2^0, \cdots, X_n^0\right)$ and $\dfrac{\Delta Z}{\Delta X_i}$ ($i = 1,2,\cdots,n$) of the finite difference method for $g\left(x_1{*}, x_2{*}, \cdots, x_n{*}\right)$ and $\left(\dfrac{\partial g}{\partial X_i}\right)^{*}$ ($i = 1,2,\cdots,n$) of the Rackwitz-Fiessler method, these two methods can be combined (Haldar and Mahadevan, 2000b).

6. Numerical Examples

To illustrate the computational procedure in Figure 1, two numerical examples, i.e., the torsionally uncoupled and coupled systems, are provided to conduct the reliability analysis of high-rise buildings under wind loads for a variety of attack angles. The results can be used to capture the dynamic effects due to the structural eccentricity.

Four types of parameters: the high-rise building model, wind load model, occupant comfort criteria and reliability analysis, are considered in this study. All parameters of the two numerical examples are the same except the eccentricity between the elastic and mass centers. For the parameters of the high-rise building model, a 40-story building ($N = 40$) with a height of 160 m is used. The geometric configuration and dynamic properties of each floor are assumed to be identical, as shown in Table I. Table II summarizes the parameters of the wind load model, where C_D and C_L are a function of ϕ (Peng, 2005). Table III lists the parameters of the occupant comfort criteria, where F is selected from the natural frequency of the first mode of each system. The parameters of the reliability analysis are illustrated in Table IV, where X_1 and X_2 are employed to simulate Ex_i and Ey_i, respectively. For both the torsionally uncoupled and coupled systems, $\mu_{X_1} = Ex_i$ and $\mu_{X_2} = Ey_i$ are given, and the probability distribution of X_1 and that of X_2 are assumed to be identical. Three types of probability distributions: the normal, lognormal and type I extreme value distributions, are used to model the uncertainties of both X_1 and X_2.

The acceleration at the top floor corner is the target of both the deterministic and reliability analyses. This is because such response is the maximum throughout the system. The relationships between the peak acceleration at corner of the 40th floor, i.e., the demand, and ϕ for the torsionally uncoupled and coupled systems are shown in Figure 5(a) and 5(b), respectively. The allowable peak acceleration independent of ϕ, i.e., the capacity, is displayed in the figures. Both the figures illustrate that the demand is comparatively lower than the capacity for each ϕ. Consequently, the occupant comfort criteria are satisfied in the two numerical examples from the viewpoint of deterministic approaches. These two figures also show that the maximum peak acceleration occurs when the wind direction is parallel to the x axis, i.e., $\phi = 0^\circ$ or 180°. The peak acceleration of the torsionally coupled system is relatively higher than that of the torsionally uncoupled system for each ϕ due to the coupled mode effects.

Table I. Parameters of the high-rise building model.

D_i	[m]	24
B_i	[m]	48
H_i	[m]	4
Ex_i	[m]	0 (TUS)
		− 1.2 (TCS)
Ey_i	[m]	0 (TUS)
		− 2.4 (TCS)
Ax_i	[m]	− 0.5
Ay_i	[m]	4.8
M_i	[kg]	10^6
I_i	[kg-m^2]	2.4×10^8
Kx_i	[N/m]	7×10^9
Ky_i	[N/m]	1.05×10^{10}
$K\theta_i$	[N/rad]	3.5×10^{12}
A_0	[s^{-1}]	0.2
A_1	[s]	0

TUS: Torsionally uncoupled system
TCS: Torsionally coupled system

Table II. Parameters of the wind load model.

α	[None]	0.36
Z_G	[m]	500
V_G	[m/s]	27.4
V_R	[m/s]	6.5
K_0	[None]	0.025
C_1	[None]	7.7
ρ	[kg/m^3]	1.23
C_D	[None]	(Peng, 2005)
C_L	[None]	(Peng, 2005)

Table III. Parameters of the occupant comfort criteria.

F	[Hz]	0.5164 (TUS)
		0.5106 (TCS)
T	[s]	600
R	[yr]	0.5

TUS: Torsionally uncoupled system
TCS: Torsionally coupled system

Table IV. Parameters of the reliability analysis.

μ_{X_1}	[m]	0 (TUS)
		− 1.2 (TCS)
μ_{X_2}	[m]	0 (TUS)
		− 2.4 (TCS)
σ_{X_1}	[m]	0.8
σ_{X_2}	[m]	0.8

TUS: Torsionally uncoupled system
TCS: Torsionally coupled system

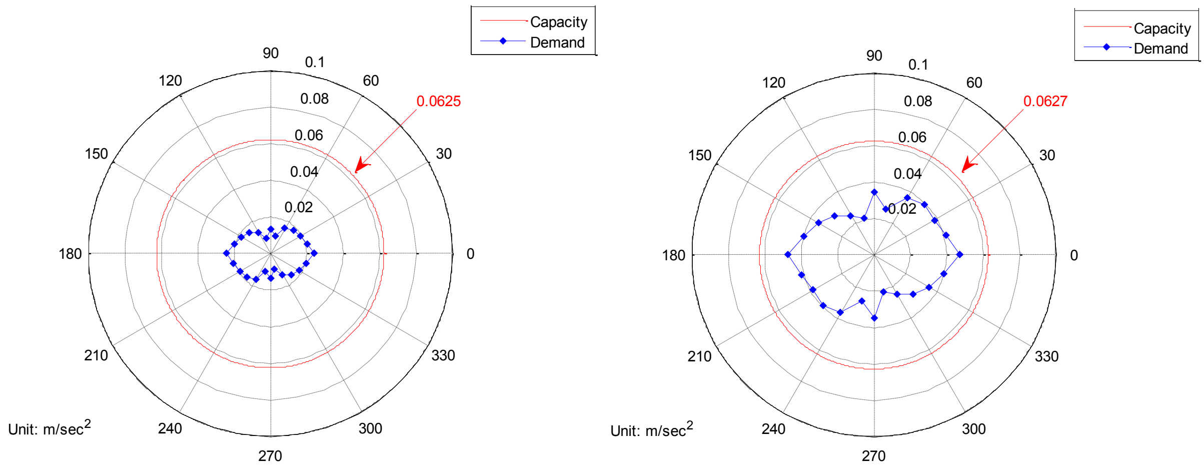

(a) Torsionally uncoupled system (b) Torsionally coupled system

Figure 5. Relationships between the peak acceleration at corner of the 40th floor and the attack angle.

The reliability analysis is conducted based on the demand and capacity obtained by the deterministic analysis. The relationships between the probability of dissatisfaction with occupant comfort criteria for three types of probability distributions of the structural eccentricity, i.e., the normal, lognormal and type I extreme value distributions, and ϕ for the torsionally uncoupled and coupled systems are shown in Figure 6(a) and 6(b), respectively. Both the figures illustrate that the probability for the case of the normal distribution is relatively higher than that for the other two cases for each ϕ . Furthermore, the probability for the case of the lognormal distribution is close to that of the type I extreme value distribution for each ϕ . The findings indicate that, compared to the lognormal and type I extreme value distributions, the normal distribution can be used to more conservatively simulate the uncertainties of the eccentricity between EC_i and MC_i in the two numerical examples from the viewpoint of probabilistic approaches. These two figures also show that the maximum probability occurs when the wind direction is parallel to the x axis, i.e., $\phi = 0^\circ$ or 180°. The probability of the torsionally coupled system is relatively higher than that of the torsionally uncoupled system for each ϕ due to the coupled mode effects. The results are in agreement with those obtained by the deterministic analysis.

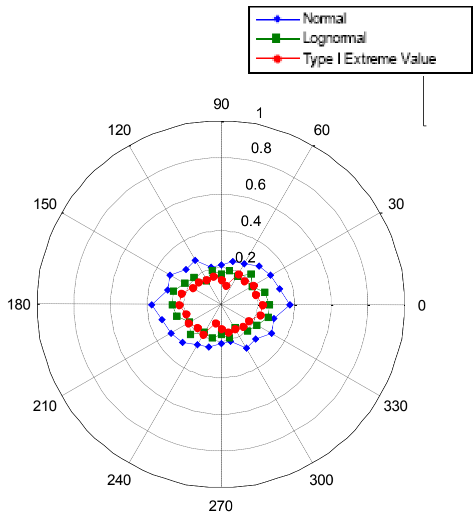

(a) Torsionally uncoupled system

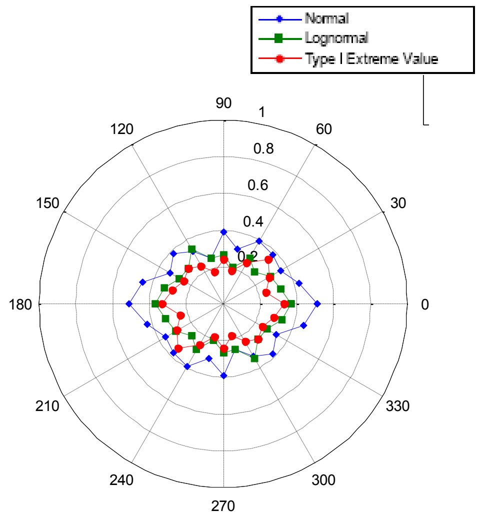

(b) Torsionally coupled system

Figure 6. Relationships between the probability of dissatisfaction with occupant comfort criteria and the attack angle.

7. Conclusions

The objective of this paper is to conduct the reliability analysis of high-rise buildings under wind loads. Two numerical examples, i.e., the torsionally uncoupled and coupled systems, are provided to capture the dynamic effects of structures with eccentricity between the elastic and mass centers. The framework of this research consists of two stages. The first stage includes two parts: the deterministic analysis of wind-induced acceleration for a variety of attack angles, i.e., the demand, and the determination of allowable acceleration based on the occupant comfort criteria for wind-excited buildings, i.e., the capacity. According to the results obtained in the first stage, the reliability analysis is conducted in the second stage, which can predict the probability of dissatisfaction with occupant comfort criteria for three types of probability distributions of the structural eccentricity, i.e., the normal, lognormal and type I extreme value distributions.

In the first stage, both the examples illustrate that the demand is comparatively lower than the capacity for each attack angle. Consequently, the occupant comfort criteria are satisfied in the two numerical examples from the viewpoint of deterministic approaches. These two examples also show that the maximum peak acceleration occurs when the wind direction is parallel to the x axis. The peak acceleration of the torsionally coupled system is relatively higher than that of the torsionally uncoupled system for each attack angle due to the coupled mode effects.

In the second stage, both the examples illustrate that the probability for the case of the normal distribution is relatively higher than that for the other two cases for each attack angle. Furthermore, the probability for the case of the lognormal distribution is close to that of the type I extreme value distribution for each attack angle. The findings indicate that, compared to the lognormal and type I extreme value distributions, the normal distribution can be used to more conservatively simulate the uncertainties of the eccentricity between the elastic and mass centers in the two numerical examples from the viewpoint of probabilistic approaches. These two examples also show that the maximum probability occurs when the wind direction is parallel to the x axis. The probability of the torsionally coupled system is relatively higher than that of the torsionally uncoupled system for each attack angle due to the coupled mode effects. The results are in agreement with those obtained by the deterministic analysis.

Acknowledgements

The authors would like to acknowledge the support of the National Science Council, Taiwan, under Grant No. NSC 98-2218-E-033-001.

References

Davenport, A. G. The Dependence of Wind Load upon Meteorological Parameters. *Proceedings of the International Research Seminar on Wind Effects on Buildings and Structures*, University of Toronto Press, Toronto, Canada, 1968.

Haldar, A. and S. Mahadevan. *Probability, Reliability, and Statistical Methods in Engineering Design*. John Wiley & Sons, Inc., New York City, New York, USA, 2000a.

Haldar, A. and S. Mahadevan. *Reliability Assessment Using Stochastic Finite Element Analysis*. John Wiley & Sons, Inc., New York City, New York, USA, 2000b.

Kan, C. L. and A. K. Chopra. Elastic Earthquake Analysis of Torsionally Coupled Multistorey Buildings. *Earthquake Engineering and Structural Dynamics*, 5(4):395-412, 1977.

Kareem, A. Lateral-Torsional Motion of Tall Buildings to Wind Loads. *Journal of Structural Engineering*, *ASCE*, 111(11):2479-2496, 1985.

Kareem, A. Dynamic Response of High-Rise Buildings to Stochastic Wind Loads. *Journal of Wind Engineering and Industrial Aerodynamics*, 42(1-3):1101-1112, 1992.

Liu, M. Y., W. L. Chiang, J. H. Hwang, and C. R. Chu. Wind-Induced Vibration of High-Rise Building with Tuned Mass Damper Including Soil-Structure Interaction. *Journal of Wind Engineering and Industrial Aerodynamics*, 96(6-7):1092-1102, 2008.

Melbourne, W. H. Probability Distributions Associated with the Wind Loading of Structures. *Civil Engineering Transactions, Institution of Engineers, Australia*, CE19(1):58-67, 1977.

Melbourne, W. H. and T. R. Palmer. Accelerations and Comfort Criteria for Buildings Undergoing Complex Motions. *Journal of Wind Engineering and Industrial Aerodynamics*, 41(1-3):105-116, 1992.

Peng, M. H. *Investigation of Wind Forces on Objects in Gusty Flow Using Hilbert-Huang Transform*. Master thesis, National Central University, Taiwan, 2005.

Rackwitz, R. and B. Fiessler. Note on Discrete Safety Checking when Using Non-Normal Stochastic Models for Basic Variables. *Load Project Working Session*, Massachusetts Institute of Technology, Cambridge, Massachusetts, USA, 1976.

Rackwitz, R. and B. Fiessler. Structural Reliability under Combined Random Load Sequences. *Computers and Structures*, 9(5):489-494, 1978.

Samali, B., J. N. Yang, and C. T. Yeh. Control of Lateral-Torsional Motion of Wind-Excited Buildings. *Journal of Engineering Mechanics*, *ASCE*, 111(6):777-796, 1985.

Simiu, E. and R. H. Scanlan. *Wind Effects on Structures: Fundamentals and Applications to Design*. Third Edition, John Wiley & Sons, Inc., New York City, New York, USA, 1996.

Wu, J. C. and J. N. Yang. LQG Control of Lateral-Torsional Motion of Nanjing TV Transmission Tower. *Earthquake Engineering and Structural Dynamics*, 29(8):1111-1130, 2000.

Yang, J. N., Y. K. Lin, and B. Samali. Coupled Motion of Wind-Loaded Multi-Story Building. *Journal of Engineering Mechanics Division*, *ASCE*, 107(EM6):1209-1226, 1981.